

Morphological imaging and T2 and T2* mapping of hip cartilage at 7 Tesla MRI under the influence of intravenous gadolinium

Andrea Lazik-Palm¹ · Oliver Kraff² · Christina Geis¹ · Sören Johst² · Juliane Goebel¹ · Mark E. Ladd^{1,2,3} · Harald H. Quick^{2,4} · Jens M. Theysohn¹

Received: 5 August 2015 / Revised: 21 January 2016 / Accepted: 25 January 2016 / Published online: 12 February 2016
© European Society of Radiology 2016

Abstract

Objectives To investigate the influence of intravenous gadolinium on cartilage T2 and T2* relaxation times and on morphological image quality at 7-T hip MRI.

Methods Hips of 11 healthy volunteers were examined at 7 T. Multi-echo sequences for T2 and T2* mapping, 3D T1 volumetric interpolated breath-hold examination (VIBE) and double-echo steady-state (DESS) sequences were acquired before and after intravenous application of gadolinium according to a delayed gadolinium-enhanced MRI of cartilage (dGEMRIC) protocol. Cartilage relaxation times were measured in both scans. Morphological sequences were assessed quantitatively using contrast ratios and qualitatively using a 4-point Likert scale. Student's *t*-test, Pearson's correlation (ρ) and Wilcoxon sign-rank test were used for statistical comparisons.

Results Pre- and post-contrast T2 and T2* values were highly correlated (T2: acetabular: $\rho=0.76$, femoral: $\rho=0.77$; T2*: acetabular: $\rho=0.80$, femoral: $\rho=0.72$). Gadolinium enhanced contrasts between cartilage and joint fluid in DESS and T1 VIBE according to the qualitative ($p=0.01$) and quantitative

($p<0.001$) analysis. The delineation of acetabular and femoral cartilage and the labrum predominantly improved with gadolinium.

Conclusions Gadolinium showed no relevant influence on T2 or T2* relaxation times and improved morphological image quality at 7 T. Therefore, morphological and quantitative sequences including dGEMRIC can be conducted in a one-stop-shop examination.

Key Points

- Hip cartilage T2 values correlate highly before and after gadolinium at 7 T
- Hip cartilage T2* values correlate highly before and after enhancement at 7 T
- Morphological hip cartilage imaging benefits from intravenous gadolinium at 7 T
- The delineation of acetabular and femoral cartilage can be improved by gadolinium
- Morphological and quantitative sequences including dGEMRIC can be combined as a one-stop-shop examination

Keywords Ultra-high-field MRI · Hip cartilage · dGEMRIC · T2 mapping · T2* mapping

✉ Andrea Lazik-Palm
andrea.lazik@uk-essen.de

¹ Department of Diagnostic and Interventional Radiology and Neuroradiology, University Hospital Essen, Hufelandstr. 55, 45147 Essen, Germany

² Erwin L. Hahn Institute for Magnetic Resonance Imaging, University of Duisburg-Essen, Essen, Germany

³ Division of Medical Physics in Radiology, German Cancer Research Center (DKFZ), Heidelberg, Germany

⁴ High-Field and Hybrid MR Imaging, University Hospital Essen, Essen, Germany

Abbreviations

MRI	Magnetic resonance imaging
T	Tesla
SD	Standard deviation
BMI	Body mass index
RF	Radio frequency
FLASH	Fast low-angle shot
DREAM	Dual refocusing echo acquisition mode
FOV	Field of view
TE	Echo time
TR	Repetition time

DESS	Double-echo steady state
VIBE	Volumetric interpolated breath-hold examination
dGEMRIC	Delayed gadolinium-enhanced MRI of cartilage
ROI	Region of interest
CR	Contrast ratio
SSFP	Steady-state free precession
FISP	Fast imaging steady precession

Introduction

Nowadays, morphological sequences in joint magnetic resonance imaging (MRI) are often accompanied by quantitative measurements [1, 2]. Among them, T2 and T2* relaxation times as well as delayed gadolinium-enhanced MRI of cartilage (dGEMRIC), a T1 mapping technique, deliver complementary information about the micromolecular cartilage structure [3, 4] and therefore give an impression of cartilage vitality. This is important in the staging of early cartilage degeneration [5] as well as in the follow-up after cartilage repair surgery [6]. However, the combination of these mapping techniques and the implementation in a clinical protocol is challenging, as dGEMRIC requires the application of intravenous contrast agent administration at least 1 h prior to the scan [7], whereas the other techniques as well as morphological imaging techniques usually do not. To implement all of these techniques into one clinical protocol without placing the patient in the scanner twice, performing all the techniques after initial contrast agent administration would be favourable. Another advantage of intravenous gadolinium is the possibility to perform an indirect arthrography, with the advantage of better visibility of the joint structures, such as the acetabular labrum [8, 9].

Cartilage imaging, especially at the hip joint, is challenging because of the thin cartilage layer, spherical shape of the hip joint and larger volume of surrounding soft tissue compared to other joints [10], which renders the positioning of dedicated surface coils as used for the knee impossible. Therefore, MR imaging with high magnetic field strength up to 7 T is favourable because of the associated inherently higher signal-to-noise ratio, with the potential for higher spatial resolution and improved tissue contrast [11] compared to lower magnetic field strength. Several authors have already shown successful morphological imaging of the hip joint at 7 T [12–15]. In a previous study, the technical feasibility and clinical applicability of quantitative MRI sequences for imaging hip cartilage at 7 T were also demonstrated [16].

Initial studies at field strengths up to 3 T have shown that the intravenous application of gadolinium does not have a relevant impact on T2 and T2* relaxation times [17, 18]. However, due to the change of T1 and T2(*) relaxivities with the magnetic field strength [19–21], the influence of

gadolinium cannot be simply transferred from high to ultra-high field strengths operating at 7 T.

The purpose of this study was to investigate the influence of intravenous gadolinium (1) on T2 and T2* relaxation times in cartilage and (2) on image quality in morphological sequences at 7-T hip MR imaging.

Materials and methods

Study population

The local institutional ethics committee approved this study, and all participants signed the informed consent. Eleven healthy volunteers [5 female, 6 male; 21–46 years, mean 27.0 years, SD 7.3 years; body mass index (BMI) 18.7–26.6 kg/m², mean 22.5 kg/m², SD 3.1 kg/m²] were included in the study after considering the defined exclusion criteria (current or past hip pain, previous hip surgeries, renal insufficiency, implants incompatible with 7-T MRI, claustrophobia).

MR system and radiofrequency shimming

Examinations were performed on a 7-T research whole-body MR system (Magnetom 7 T, Siemens Healthcare GmbH, Germany) using an in-house developed eight-channel radiofrequency (RF) transmit/receive coil consisting of two arrays with four elements each placed ventrally and dorsally on the pelvis [22].

Unilateral hip imaging was performed by applying the second-order circularly polarised (CP2+) RF transmit mode utilising fixed-phase increments of 90° between the eight transmit channels as a fixed RF shim setting for all subjects to achieve RF signal homogenisation across the volume of interest. This RF mode had previously proved superior to individual RF shimming in hip imaging at 7 T in terms of workflow and maximum allowed input power in compliance with safety guidelines [14]. A 3D fast low-angle shot (FLASH) sequence was used to verify the successful shift of signal dropouts medially away from the hip joint prior to the study as reported previously [16]. Additionally, maps of the flip angle distribution were obtained by fast B₁⁺ mapping using dual refocusing echo acquisition mode (DREAM) [23, 24] and utilised to adjust the transmit voltages in the quantitative imaging sequences as described previously [16].

Imaging protocol

To minimise the influences of mechanical joint load on T2 and T2* relaxation times, volunteers rested for at least half an hour prior to the scan. Multi-contrast spin-echo and gradient-echo sequences with five echoes each were applied for T2 and T2* mapping in the sagittal view [field

of view (FOV) $160 \times 160 \text{ mm}^2$, matrix 320×320 , slice thickness 2.5 mm]. Echo times (TE) used were 10.1, 20.2, 30.3, 40.4 and 50.5 ms for T2 mapping [repetition time (TR) 1500 ms] and 3.06, 8.0, 12.94, 17.88 and 22.82 ms for T2* mapping (TR 130 ms). Further sequence parameters are given in Table 1. Colour-coded maps were calculated manually (Syngo MapIt, Siemens Healthcare GmbH, Germany) using Syngo MeanCurve (Siemens Healthcare GmbH, Germany) after reviewing the consistency of signal decrease with TE. In case of a non-consistent signal decrease, images from the first echo were not considered for calculating the map.

For morphological imaging, two high-resolution 3D sequences in sagittal orientation were used: first, an isotropic double-echo steady-state (DESS) sequence (TR 11 ms, TE 4.1 ms, FOV $190 \times 190 \text{ mm}^2$, matrix 256×256); second, a T1 volumetric interpolated breath-hold examination (VIBE) sequence (TR 11 ms, TE 4.17 ms, FOV $200 \times 200 \text{ mm}^2$, matrix 512×512). Further sequence parameters are given in Table 1.

After the initial scan, the volunteers received Gd-DTPA²⁻ intravenously (Magnevist, Bayer Healthcare, Leverkusen, Germany) with a 0.2 mmol/kg body weight concentration according to a protocol for delayed gadolinium-enhanced MRI of cartilage (dGEMRIC) [7] and were subsequently asked to walk for ½ h. After another ½ h of rest, volunteers were repositioned in the MR system to acquire the same sequences as applied previously.

MRI evaluation

Relaxation times were measured prior to ($T2_0$, $T2^*_0$) and after contrast agent administration ($T2_{Gd}$, $T2^*_{Gd}$) by manually drawing regions of interest (ROIs) in five defined regions each

in acetabular and femoral cartilage: in a slice showing the central region of the femoral head, three ROIs were placed centrally as well as ventrally and dorsally. In the next (distance: 5 mm) or next but one (distance: 10 mm) slice laterally and medially each, two additional ROIs were placed centrally (Fig. 1). The distance from the central slice was chosen dependent on the size of the femoral head and was kept constant intra- individually.

For measuring contrast ratios between cartilage and adjacent structures in the morphological sequences, ROIs were placed in the joint fluid and the subchondral bone as well as in the above-mentioned cartilage regions. Afterwards, contrast ratios were calculated by $CR = (S_{\text{Cartilage}} - S_{\text{Reference}}) / (S_{\text{Cartilage}} + S_{\text{Reference}})$, with $S_{\text{Cartilage}}$ being the signal in the individual cartilage regions and $S_{\text{Reference}}$ being the signal of the joint fluid or the subchondral bone.

A qualitative analysis, which was done in consensus by two radiologists, focused on the subjective delineation of acetabular and femoral cartilage (4-point scale: 1 = not delineable; 2 = partly delineable; 3 = largely delineable; 4 = fully delineable) in the calculated relaxation time maps as well as in the morphological sequences, both prior to and after contrast agent administration. Furthermore, the morphological sequences were evaluated in consensus regarding the homogeneity of the signal in the hip joint region (3-point scale: 1 = severe heterogeneities; 2 = moderate heterogeneities; 3 = no heterogeneities), artefacts affecting image quality (3-point-scale: 1 = severe artefacts; 2 = moderate artefacts; 3 = no artefacts), the subjective contrast between cartilage and joint fluid or subchondral bone (4-point scale: 1 = no contrast; 2 = moderate contrast; 3 = good contrast; 4 = excellent contrast) and regarding the assessability of the acetabular labrum (1 = not assessable; 2 = hardly assessable; 3 = fairly assessable; 4 = well assessable).

Table 1 Sequence parameters for 7-T hip MR imaging

	T2 mapping	T2* mapping	DESS	T1 VIBE
TR (ms)	1500	130	11	11
TE (ms)	10.1–50.5	3.06–22.82	4.1	4.17
FOV (mm)	160	160	190	200
In-plane resolution (mm^2)	0.5×0.5	0.5×0.5	0.7×0.7	0.4×0.4
Slice thickness (mm)	2.5	2.5	0.7	0.8
Distance factor (%)	100	100	0	0
Number of slices	5	5	128	104
Bandwidth (Hz/pixel)	401	500	391	130
PAT	2 (GRAPPA)	None	2 (GRAPPA)	2 (GRAPPA)
Averages	1	2	1	1
Acquisition time (min)	4:53	2:06	5:12	5:57

DESS = double-echo steady state; VIBE = volumetric interpolated breath-hold examination; TR = repetition time; TE = echo time; FOV = field of view; PAT = parallel acquisition technique; GRAPPA = generalised autocalibration with partially parallel acquisition. All sequences were applied in sagittal orientation with phase-encoding direction in anterior-posterior direction and a slice resolution of 100 %

Statistical analysis

Mean values with standard deviations (SDs) were calculated for all parameters. Statistical analysis was performed using SPSS Statistics 19 (IBM, USA). Differences between contrast ratios of unenhanced (CR_0) and contrast-enhanced (CR_{Gd}) DESS and T1 sequences were calculated using Student's t-test. Differences between pre- and post-contrast T2 and $T2^*$ values were evaluated by Student's t-test for two dependent samples, and correlations between them by Pearson's correlation, where the correlation coefficient ρ as well as its 95 % confidence interval (95 % CI) were calculated. Agreements between the pre- and post-contrast measurements were visualised using Bland-Altman plots [25]. Differences regarding the qualitative data were calculated using Wilcoxon sign rank tests.

Results

Gadolinium does not influence T2 and $T2^*$ relaxation times

Mean size of the evaluated ROIs was 210 pixels. $T2_0$ and $T2_{Gd}$ relaxation times did not differ for either acetabular or femoral cartilage [acetabular: 44.5 ± 8.2 ms (range: 31–65 ms) vs. 43.2 ± 7.7 ms (range: 31–65 ms), $p=0.101$; femoral: 40.7 ± 7.9 ms (range: 24–56 ms) vs. 40.1 ± 6.7 ms (range: 27–60 ms), $p=0.347$] and showed a high correlation (acetabular:

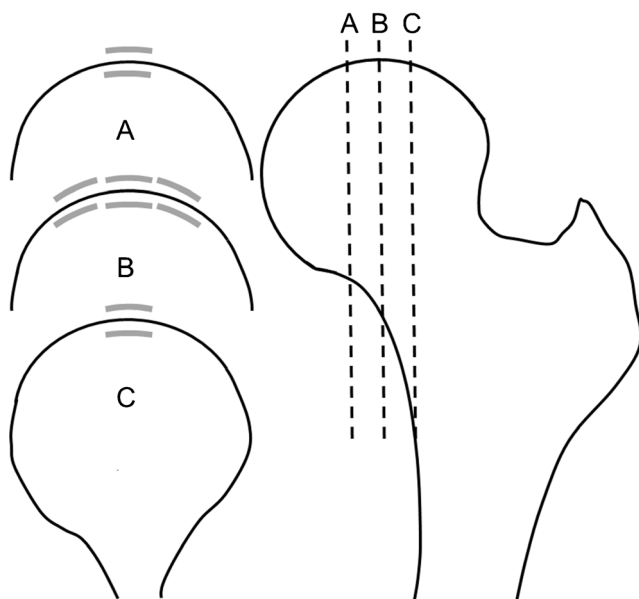


Fig. 1 Schematic view of the analysed cartilage regions (grey) in the sagittal relaxation maps. (b) Three ROIs were placed (centrally, ventrally, dorsally) in the central slice, each in the acetabular and femoral cartilage. In slices 5–10 mm medial (a) and lateral (c) to the central slice, one ROI was placed centrally in both the acetabular and femoral cartilage

$\rho=0.76$, 95 % CI 0.62–0.86, femoral: $\rho=0.77$, 95 % CI 0.63–0.88). The good agreement of the measurements is shown in Fig. 2a. A trend towards slightly higher $T2^*_0$ values compared to the values of $T2^*_{Gd}$ was observed in acetabular cartilage [15.2 ± 4.1 ms (range: 9–29 ms) vs. 14.5 ± 3.8 ms (range 8–26 ms), $p=0.048$] but not in femoral cartilage [15.3 ± 3.8 ms (range: 9–24 ms) vs. 14.7 ± 3.8 ms (range: 9–24 ms), $p=0.107$]. A high correlation between $T2^*_0$ and $T2^*_{Gd}$ in acetabular cartilage ($\rho=0.80$, 95 % CI 0.67–0.88) as well as in femoral cartilage ($\rho=0.72$, 95 % CI 0.56–0.83) was found, and good agreement was shown in the Bland-Altman plot (Fig. 2b).

The delineation of femoral and acetabular cartilage was not affected by the administration of contrast agent in either the T2 maps [$T2_0$: 3.0 ± 1 (range: 1–4) vs. $T2_{Gd}$: 3.2 ± 0.9 (range: 2–4), $p=0.157$] or $T2^*$ maps [$T2^*_0$: 3.2 ± 0.4 (range: 3–4) vs. $T2^*_{Gd}$: 3.2 ± 0.4 (range: 3–4), $p=1.0$].

Gadolinium enhances the contrast between cartilage and adjacent structures in DESS and T1 VIBE

The contrast ratio between cartilage and subchondral bone increased slightly after contrast agent administration in both T1 VIBE [$CR_0=0.73 \pm 0.06$ (range: 0.53–0.84), $CR_{Gd}=0.74 \pm 0.07$ (range: 0.56–0.85), $p=0.029$] and DESS [$CR_0=0.60 \pm 0.09$ (range 0.34–0.75), $CR_{Gd}=0.64 \pm 0.09$ (range: 0.39–0.79), $p<0.001$]. The contrast ratio between cartilage and joint fluid increased clearly after contrast agent administration in both T1 VIBE [$CR_0=0.11 \pm 0.10$ (range 0.09–0.33), $CR_{Gd}=0.32 \pm 0.07$ (range 0.13–0.55), $p<0.001$] and DESS [$CR_0=0.24 \pm 0.07$ (range: 0.02–0.41), $CR_{Gd}=0.36 \pm 0.08$ (range: 0.16–0.56), $p<0.001$]. Therefore, the highest improvement in contrast by the application of gadolinium was observed between joint fluid and cartilage in T1 VIBE (Fig. 2c).

The qualitative analysis (Table 2) also revealed the best contrast between cartilage and joint fluid in contrast-enhanced T1 VIBE (3.4 ± 0.8 points), with clear improvement compared to unenhanced T1 VIBE (1.8 ± 1.1 points, $p=0.01$). The subjective contrast between cartilage and joint fluid in DESS increased only slightly after contrast agent administration (2.8 ± 0.9 vs. 2.4 ± 0.8 points, $p=0.129$). No subjective difference was observed prior to and after contrast agent administration regarding the contrast between cartilage and subchondral bone in either DESS (both 3.7 ± 0.5 points, $p=1$) or T1 VIBE (3.9 ± 0.3 vs. 4.0 ± 0.0 points, $p=0.32$).

Gadolinium enhances the subjective delineation of acetabular and femoral cartilage in T1 VIBE but not in DESS

The contrast-enhanced T1 VIBE sequence showed a clearly improved score for the delineation of femoral and acetabular

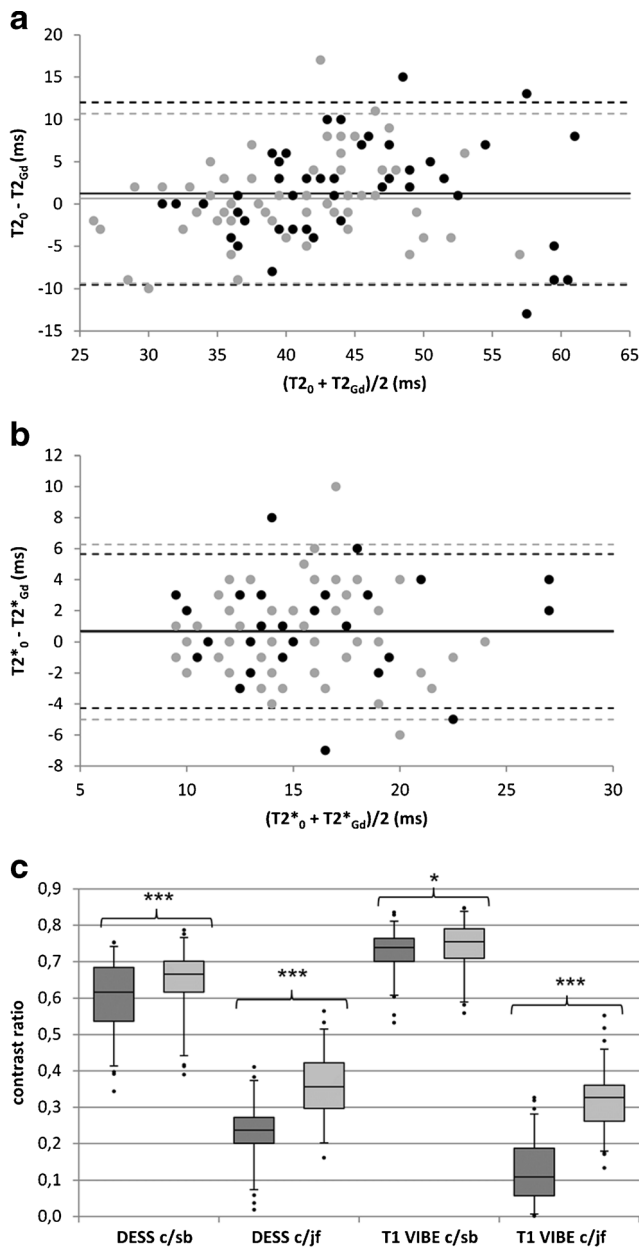


Fig. 2 **a** Bland-Altman plot showing the agreement between pre- ($T2_0$) and post-contrast ($T2_{Gd}$) measurements for T2 relaxation times of acetabular (black) and femoral (grey) cartilage. The horizontal solid lines represent the mean difference between the two measurements (acetabular: 1.24 ms; femoral: 0.65 ms). The horizontal dashed lines represent the 95 % limits of agreement. **b** Bland-Altman plot showing the agreement between pre- ($T2^*_0$) and post-contrast ($T2^*_{Gd}$) measurements for T2* relaxation times of acetabular (black) and femoral (grey) cartilage. The horizontal solid lines (overlapping) represent the mean difference between the two measurements (acetabular: 0.69 ms; femoral: 0.63 ms). The horizontal dashed lines represent the 95 % limits of agreement. **c** Improvement of contrast ratios between cartilage (c) and subchondral bone (sb) and between cartilage and joint fluid (jf) in DESS and T1 VIBE after contrast agent administration [dark grey = contrast ratios of unenhanced scans (CR_0), light grey = contrast ratios of contrast-enhanced scans (CR_{Gd})]. The boxplot represents the 2.5th percentile (bottom end of the whisker), the first quartile (bottom of the box), the sample median (line through the box), the third quartile (top of the box) and the 97.5th percentile (top end of the whisker). The dots indicate outliers. * $p < 0.05$, *** $p < 0.001$

cartilage compared to the unenhanced images (3.2 ± 0.6 vs. 2.2 ± 0.9 points, $p = 0.02$) (Table 2). However, subjective delineation of acetabular and femoral cartilage decreased after contrast agent administration in DESS (1.9 ± 0.3 vs. 2.6 ± 0.7 points, $p = 0.01$) (Fig. 3, Table 2). The delineation in the unenhanced images did not differ between DESS and T1 VIBE ($p = 0.129$), but did in the contrast-enhanced images ($p = 0.002$) (Fig. 3, Table 2).

Gadolinium enhances the assessability of the acetabular labrum

The assessability of the acetabular labrum clearly increased after contrast agent administration in DESS (2.9 ± 0.7 vs. 2.0 ± 0.8 points, $p = 0.01$) and even more in T1 VIBE (3.1 ± 1.0 vs. 1.8 ± 1.0 points, $p = 0.01$) (Fig. 4, Table 2).

Seven-Tesla MR imaging delivers excellent image quality for morphological cartilage imaging in the hip

No severe signal heterogeneities were observed in the morphological sequences. In one volunteer, moderate signal heterogeneities in the dorsal part of the hip joint region were noticed, which were consistent in DESS and T1 VIBE prior to and after contrast agent administration, resulting in an overall score of 2.09 ± 0.3 points for all volunteers (Table 2). Image quality was partly reduced by the appearance of pulsation artefacts originating from the inguinal vessels. This was most pronounced in DESS (both prior to and after contrast agent administration), with a mean score for artefacts of 1.9 ± 0.8 points, followed by contrast-enhanced T1 VIBE (2.5 ± 0.5 points) (Table 2). Unenhanced T1 VIBE showed the fewest pulsation artefacts (2.7 ± 0.5 points) (Table 2). No other artefacts were observed. Exemplary images with the best and worst ratings are shown in Fig. 5.

Discussion

This initial study on the influence of intravenously applied gadolinium on T2 and T2* relaxation times at 7-T MRI shows that these relaxation times are not affected by the use of a contrast agent in a clinically relevant manner, which is in line with data previously reported for MRI at lower magnetic field strengths [18, 26]. Although paramagnetic contrast agents shorten not only T1 but to a lesser degree also T2 and T2*, the magnitude of this effect does not seem to be clinically relevant when imaging articular cartilage [27, 28], especially when concentrations of $Gd-DTPA^{2-}$ typical for a dGEMRIC protocol are used [29]. Based on the current results, the T2 and/or T2* mapping technique can be easily applied in combination with contrast-enhanced T1 mapping according to a dGEMRIC protocol at 7-T MRI, delivering a comprehensive

Table 2 Results of the qualitative analysis of the morphological sequences regarding (1) the subjective delineation of acetabular and femoral cartilage (4-point scale: 1 = not delineable; 2 = partly delineable; 3 = largely delineable; 4 = fully delineable), (2) the homogeneity of the signal in the hip joint region (3-point scale: 1 = severe inhomogeneities; 2 = moderate inhomogeneities; 3 = no inhomogeneities), (3) artefacts affecting image quality (3-point-scale: 1 = severe artefacts; 2 = moderate

artefacts; 3 = no artefacts), (4) the subjective contrast between cartilage and joint fluid or subchondral bone (4-point scale: 1 = no contrast; 2 = moderate contrast; 3 = good contrast; 4 = excellent contrast) and (5) the assessability of the acetabular labrum (1 = not assessable; 2 = hardly assessable; 3 = fairly assessable; 4 = well assessable). Results are shown as mean \pm standard deviation

	T1 VIBE without Gd	T1 VIBE with Gd	<i>p</i>	DESS without Gd	DESS with Gd	<i>p</i>
Delineation of acetabular/femoral cartilage	2.2 \pm 0.9	3.2 \pm 0.6	0.02	2.6 \pm 0.7	1.9 \pm 0.3	0.01
Signal homogeneity	2.09 \pm 0.3	2.09 \pm 0.3	1.0	2.09 \pm 0.3	2.09 \pm 0.3	1.0
Artefacts	2.7 \pm 0.5	2.5 \pm 0.5	0.16	1.9 \pm 0.8	1.9 \pm 0.8	1.0
Subjective contrast between cartilage and joint fluid	1.8 \pm 1.1	3.4 \pm 0.8	0.01	2.4 \pm 0.8	2.8 \pm 0.9	0.13
Subjective contrast between cartilage and subchondral bone	3.9 \pm 0.3	4.0 \pm 0.0	0.32	3.7 \pm 0.5	3.7 \pm 0.5	1.0
Assessability of the acetabular labrum	1.8 \pm 1.0	3.1 \pm 1.0	0.01	2.9 \pm 0.7	2.0 \pm 0.8	0.01

Gd = Gadolinium

quantitative cartilage imaging protocol with simplified workflow.

To implement morphological sequences in this protocol as well, it would be favourable to acquire these only once after initial contrast agent application, without degradation of image quality and assessability of the joint structures. According to our results, a preceding intravenous contrast agent application even enhances image quality in T1 VIBE, with better delineation of femoral and acetabular cartilage as well as

better assessability of the acetabular labrum, as known from studies on direct and indirect MR arthrography [30, 31]. This is based on the transfer of the contrast medium molecules from the blood into the joint cavity [32] and underlined by the accentuated contrast ratios between cartilage and joint fluid. As the contrast between cartilage and subchondral bone is already high without contrast enhancement, the contrast ratios between these two tissues were only slightly improved after contrast agent administration.

Fig. 3 Sagittal views of the left hip of two healthy volunteers. In the first volunteer, the delineation of femoral and acetabular cartilage improves in T1 VIBE from 1 point in the unenhanced scan (a) to 4 points in the contrast-enhanced scan (b). In another volunteer, the delineation of femoral and acetabular cartilage decreases in DESS from 4 points (c, unenhanced) to 2 points (d, contrast enhanced)

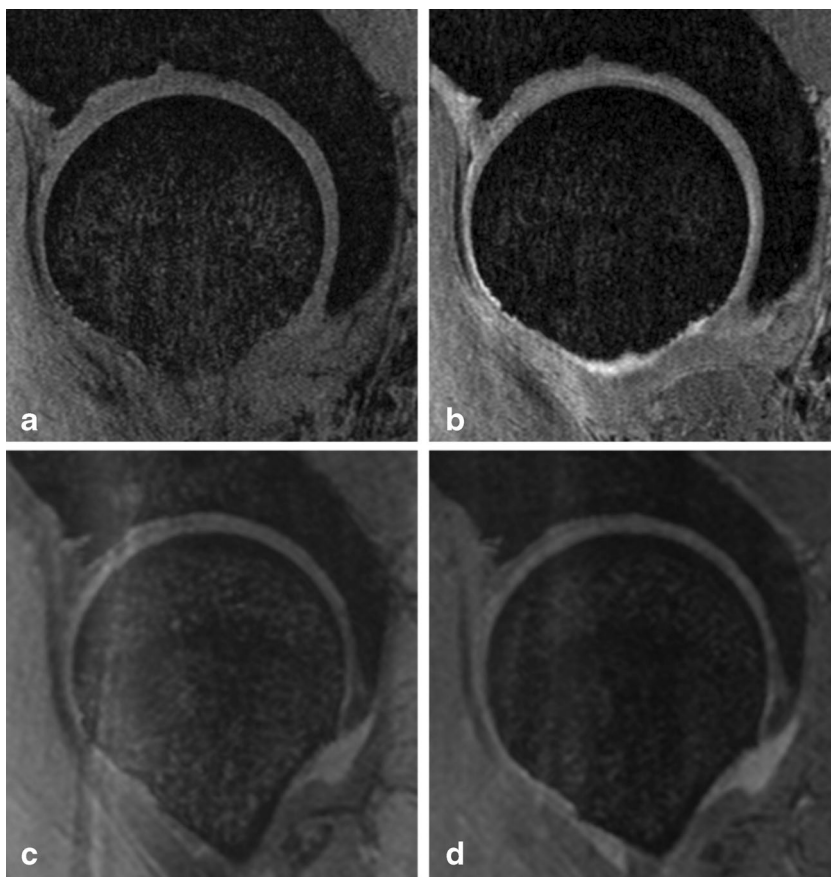
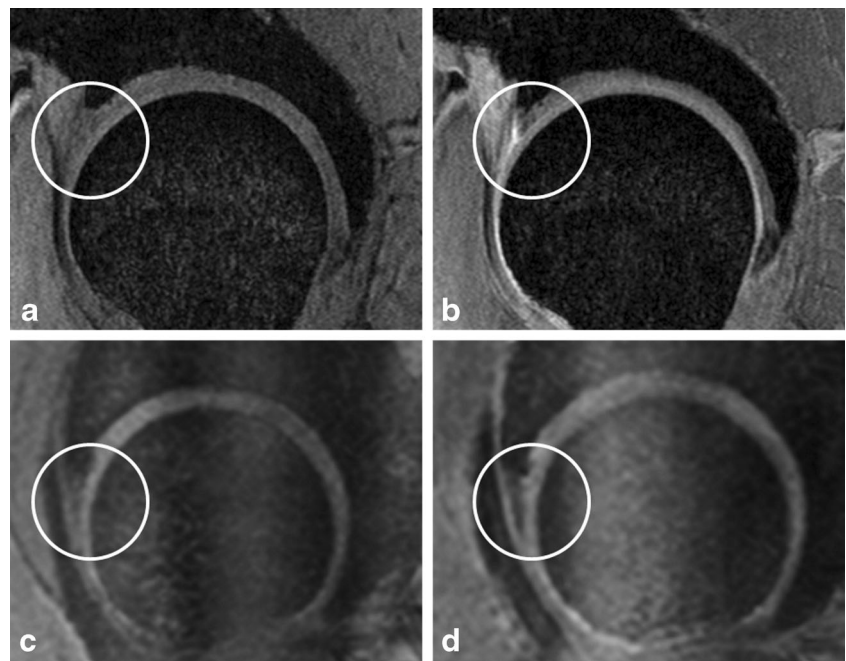


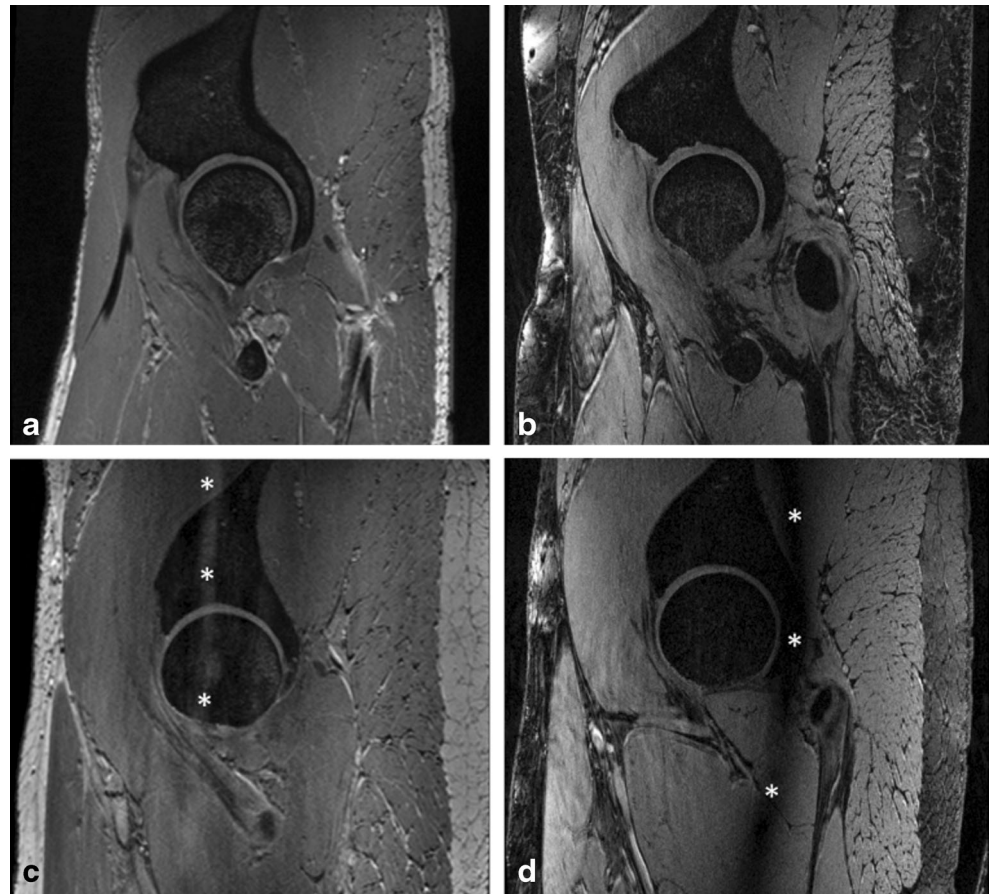
Fig. 4 Sagittal views of the left hip of a healthy volunteer in T1 VIBE (a, b) and of another healthy volunteer in DESS (c, d). The assessability of the acetabular labrum (evaluated region marked by the white circle) clearly increases after contrast agent administration from 1 point in both unenhanced scans (a, c) to 4 points in T1 VIBE and 3 points in DESS (b, d)



The DESS image is a sum of squares combination of two steady-state free precession (SSFP) echoes, FISP (fast imaging steady precession) and PSIF (reversed FISP). The PSIF part leads to a high T2 contrast, whereas the FISP contrast is

dominated by the T1/T2 ratio and will hence be influenced in part by the administration of gadolinium. Although DESS sequences are among the most favourable techniques for high-resolution 3D cartilage imaging [14, 33] and have been

Fig. 5 Exemplary images with best rated quality in DESS (a) and in T1 VIBE (b) and examples of worst ratings regarding artefacts (c, pulsation artefacts in DESS, marked with stars) and signal heterogeneity (d, signal loss in T1 VIBE, marked with stars)



used in combination with MR arthrography in several studies [34, 35], the influence of contrast agents on image contrast in DESS has, to our knowledge, never been studied before. This study shows that the use of intravenous gadolinium is advantageous not only in T1 but also in DESS to improve contrast ratios between cartilage and surrounding tissues and to better delineate the acetabular labrum, when a slight subjective degradation of acetabular and femoral cartilage delineation is accepted. However, as only healthy volunteers were included in the study, it remains unclear whether the contrast agent administration may mask pathologies such as signal alterations in the acetabular labrum or bone marrow oedema-like lesions. This has to be taken into account when further studies on patients are conducted. Furthermore, the potential influence of gadolinium has to be kept in mind when different T2 mapping techniques, such as the triple-echo steady-state sequence, which is a derivative of the DESS sequence, are used [36].

A limitation of the study design is the use of a consensus rating for the qualitative analysis instead of using a rating scheme of two independent raters. However, as there are no standards regarding image quality, since the application of the evaluated techniques remains limited to a few studies so far, we have found this rating more appropriate for 7 T.

A further limitation of our study is the absence of T2- and proton-density-weighted fast spin-echo sequences, which are favourable for morphological cartilage imaging [37]. Fast spin-echo techniques using a large number of RF refocusing pulses with high flip angles of 180° are limited at ultra-high-field MRI because of their increased power deposition in the examined tissue and limited available peak RF power. Therefore, the DESS sequence has been chosen in this study as a reasonable alternative for morphological cartilage imaging [38].

Seven Tesla not only offers the possibility of better image quality, but also the application of dedicated techniques, which are more difficult to perform at lower field strengths: for biochemical cartilage imaging, sodium imaging and glycosaminoglycan chemical exchange saturation transfer (gagCEST) promise to be valuable alternatives to dGEMRIC without the need of contrast agent administration [39]. Also diffusion tensor imaging has recently proven its feasibility and reproducibility for the diagnosis of osteoarthritis [40]. However, these techniques are in their early technical development even in 3-T systems [41] and have not yet been fully evaluated for clinical use, especially in patients after cartilage repair surgery [42]. As the present work should pave the way to conducting comparative field strength studies in patients with clinically applicable protocols, these demanding techniques may be of interest in future studies.

In conclusion, this study shows that at 7-T MR imaging T2 and T2* relaxation times are largely unchanged even after intravenous contrast agent administration and that morphological sequences benefit from intravenous gadolinium. These

results pave the way to implementing dGEMRIC in a comprehensive 7-T MRI hip cartilage protocol combining morphological and quantitative MR sequences in a one-stop-shop examination.

Acknowledgments The authors thank Desmond Tse (Maastricht University, The Netherlands) for providing the source code of the DREAM sequence.

This work was supported by a research grant (“IFORES”) from the University Duisburg-Essen, Germany, awarded to the first author. Different results of the same study population have already been published in “7 Tesla quantitative hip MRI: T1, T2 and T2* mapping of hip cartilage in healthy volunteers” (Lazik A et al., *Eur Radiol.* 2015 Aug 28. DOI 10.1007/s00330-015-3964-0).

The scientific guarantor of this publication is Dr. med. Andrea Lazik-Palm. The authors of this manuscript declare no relationships with any companies, whose products or services may be related to the subject matter of the article. No complex statistical methods were necessary for this paper.

Institutional Review Board approval was obtained. Written informed consent was obtained from all subjects (patients) in this study. Methodology: prospective, experimental, performed at one institution.

References

1. Binks DA, Hodgson RJ, Ries ME et al (2013) Quantitative parametric MRI of articular cartilage: a review of progress and open challenges. *Br J Radiol* 86:20120163
2. Rogers AD, Payne JE, Yu JS (2013) Cartilage imaging: a review of current concepts and emerging technologies. *Semin Roentgenol* 48: 148–157
3. Bashir A, Gray ML, Burstein D (1996) Gd-DTPA2- as a measure of cartilage degradation. *Magn Reson Med* 36:665–673
4. Liess C, Lusse S, Karger N, Heller M, Gluer CC (2002) Detection of changes in cartilage water content using MRI T2-mapping in vivo. *Osteoarthr Cartil* 10:907–913
5. Gold SL, Burge AJ, Potter HG (2012) MRI of hip cartilage: joint morphology, structure, and composition. *Clin Orthop Relat Res* 470:3321–3331
6. Nieminen MT, Nissi MJ, Mattila L, Kiviranta I (2012) Evaluation of chondral repair using quantitative MRI. *J Magn Reson Imaging* 36:1287–1299
7. Burstein D, Velyvis J, Scott KT et al (2001) Protocol issues for delayed Gd(DTPA)(2-)-enhanced MRI (dGEMRIC) for clinical evaluation of articular cartilage. *Magn Reson Med* 45:36–41
8. Morrison WB (2005) Indirect MR arthrography: concepts and controversies. *Semin Musculoskelet Radiol* 9:125–134
9. Petchprapa CN, Rybak LD, Dunham KS, Lattanzi R, Recht MP (2015) Labral and cartilage abnormalities in young patients with hip pain: accuracy of 3-Tesla indirect MR arthrography. *Skelet Radiol* 44:97–105
10. Kijowski R (2010) Clinical cartilage imaging of the knee and hip joints. *AJR Am J Roentgenol* 195:618–628
11. Krug R, Stehling C, Kelley DA, Majumdar S, Link TM (2009) Imaging of the musculoskeletal system in vivo using ultra-high field magnetic resonance at 7 T. *Investig Radiol* 44:613–618
12. Chang G, Deniz CM, Honig S et al (2014) MRI of the hip at 7T: feasibility of bone microarchitecture, high-resolution cartilage, and clinical imaging. *J Magn Reson Imaging* 39:1384–1393
13. Ellermann J, Goerke U, Morgan P et al (2012) Simultaneous bilateral hip joint imaging at 7 Tesla using fast transmit B(1) shimming

- methods and multichannel transmission - a feasibility study. *NMR Biomed* 25:1202–1208
14. Theysohn JM, Kraff O, Orzada S et al (2013) Bilateral hip imaging at 7 Tesla using a multi-channel transmit technology: initial results presenting anatomical detail in healthy volunteers and pathological changes in patients with avascular necrosis of the femoral head. *Skelet Radiol* 42:1555–1563
 15. Theysohn JM, Kraff O, Theysohn N et al (2014) Hip imaging of avascular necrosis at 7 Tesla compared with 3 Tesla. *Skelet Radiol* 43:623–632
 16. Lazik A, Theysohn JM, Geis C et al (2015) 7 Tesla quantitative hip MRI: T1, T2 and T2* mapping of hip cartilage in healthy volunteers. *Eur Radiol*. doi:10.1007/s00330-015-3964-0
 17. Nissi MJ, Mortazavi S, Hughes J, Morgan P, Ellermann J (2015) T2* relaxation time of acetabular and femoral cartilage with and without intraarticular gadopentetate dimeglumine in patients with femoroacetabular impingement. *AJR Am J Roentgenol* 204:W695–W700
 18. Verschueren J, Tiel J, Reijman M et al (2014) T2 relaxation times of knee articular cartilage in osteoarthritis patients are not influenced by gadolinium contrast agent. *Radiological Society of North America 2014 Scientific Assembly and Annual Meeting, Chicago*
 19. Fries P, Morelli JN, Lux F, Tillement O, Schneider G, Buecker A (2014) The issues and tentative solutions for contrast-enhanced magnetic resonance imaging at ultra-high field strength. *Wiley Interdiscip Rev Nanomed Nanobiotechnol* 6:559–573
 20. Kalavagunta C, Michaeli S, Metzger GJ (2014) In vitro Gd-DTPA relaxometry studies in oxygenated venous human blood and aqueous solution at 3 and 7 T. *Contrast Media Mol Imaging* 9:169–176
 21. Noebauer-Huhmann IM, Szomolanyi P, Juras V, Kraff O, Ladd ME, Trattnig S (2010) Gadolinium-based magnetic resonance contrast agents at 7 Tesla: in vitro T1 relaxivities in human blood plasma. *Investig Radiol* 45:554–558
 22. Orzada S, Quick HH, Ladd ME et al (2009) A flexible 8-channel transmit/receive body coil for 7 T human imaging. *Proc Intl Soc Mag Reson Med* 17, Hawaii, USA, pp 2999
 23. Nehrke K, Bornert P (2012) DREAM—a novel approach for robust, ultrafast, multislice B(1) mapping. *Magn Reson Med* 68:1517–1526
 24. Kraff O, Lazik A, Brenner D et al (2015) In vivo comparison of B1 mapping techniques for hip joint imaging at 7 Tesla. *Proc Intl Soc Mag Reson Med* 23, Toronto, Canada
 25. Bland JM, Altman DG (1986) Statistical methods for assessing agreement between two methods of clinical measurement. *Lancet* 1:307–310
 26. Mortazavi S, Nissi M, Hughes J, Morgan P, Ellermann J (2014) T2* relaxation time of acetabular and femoral cartilage with and without intra-articular Gd-DTPA2- in hip FAI patients. *Radiological Society of North America 2014 Scientific Assembly and Annual Meeting, Chicago*
 27. Nieminen MT, Menezes NM, Williams A, Burstein D (2004) T2 of articular cartilage in the presence of Gd-DTPA2. *Magn Reson Med* 51:1147–1152
 28. Kurkijarvi JE, Nissi MJ, Rieppo J et al (2008) The zonal architecture of human articular cartilage described by T2 relaxation time in the presence of Gd-DTPA2. *Magn Reson Imaging* 26:602–607
 29. May DA, Pennington DJ (2000) Effect of gadolinium concentration on renal signal intensity: An in vitro study with a saline bag model. *Radiology* 216:232–236
 30. Sutter R, Zubler V, Hoffmann A et al (2014) Hip MRI: how useful is intraarticular contrast material for evaluating surgically proven lesions of the labrum and articular cartilage? *AJR Am J Roentgenol* 202:160–169
 31. Vahlensieck M, Peterfy CG, Wischer T et al (1996) Indirect MR arthrography: optimization and clinical applications. *Radiology* 200:249–254
 32. Vahlensieck M, Sommer T, Textor J et al (1998) Indirect MR arthrography: techniques and applications. *Eur Radiol* 8:232–235
 33. Peterfy CG, Schneider E, Nevitt M (2008) The osteoarthritis initiative: report on the design rationale for the magnetic resonance imaging protocol for the knee. *Osteoarthr Cartil* 16:1433–1441
 34. Lee MJ, Motamedi K, Chow K, Seeger LL (2008) Gradient-recalled echo sequences in direct shoulder MR arthrography for evaluating the labrum. *Skelet Radiol* 37:19–25
 35. Schmitt R, Christopoulos G, Meier R et al (2003) Direct MR arthrography of the wrist in comparison with arthroscopy: a prospective study on 125 patients. *Röfo* 175:911–919
 36. Juras V, Bohndorf K, Heule R et al (2015) A comparison of multi-echo spin-echo and triple-echo steady-state T2 mapping for in vivo evaluation of articular cartilage. *Eur Radiol*. doi:10.1007/s00330-015-3979-6
 37. Paunipagar BK, Rasalkar D (2014) Imaging of articular cartilage. *Indian J Radiol Imaging* 24:237–248
 38. Roemer FW, Kwok CK, Hannon MJ et al (2011) Semiquantitative assessment of focal cartilage damage at 3T MRI: a comparative study of dual echo at steady state (DESS) and intermediate-weighted (IW) fat suppressed fast spin echo sequences. *Eur J Radiol* 80:e126–e131
 39. Schmitt B, Zbyn S, Stelzener D et al (2011) Cartilage quality assessment by using glycosaminoglycan chemical exchange saturation transfer and ²³Na MR imaging at 7 T. *Radiology* 260:257–264
 40. Raya JG, Dettmann E, Notohamiprodjo M, Krasnokutsky S, Abramson S, Glaser C (2014) Feasibility of in vivo diffusion tensor imaging of articular cartilage with coverage of all cartilage regions. *Eur Radiol* 24:1700–1706
 41. Zbyn S, Mlynarik V, Juras V, Szomolanyi P, Trattnig S (2015) Evaluation of cartilage repair and osteoarthritis with sodium MRI. *NMR Biomed*. doi:10.1002/nbm.3280
 42. Rehnitz C, Kupfer J, Streich NA et al (2014) Comparison of biochemical cartilage imaging techniques at 3 T MRI. *Osteoarthr Cartil* 22:1732–1742